Rapid ballistic readout for flux qubits

Dmitri V. Averin, Kristian Rabenstein, and Vasili K. Semenov
Department of Physics and Astronomy, Stony Brook University, SUNY, Stony Brook, New York 11794-3800, USA
(Received 27 October 2005; revised manuscript received 17 January 2006; published 8 March 2006)

We suggest a magnetic flux detector that can be optimized with respect to the measurement back action, e.g., for the situation of quantum measurements. The detector is based on manipulation of ballistic motion of individual fluxons in a Josephson transmission line (JTL), with the output information contained in either probabilities of fluxon transmission and reflection, or time delay associated with the fluxon propagation through the JTL. We calculate the detector characteristics of the JTL and derive equations for conditional evolution of the measured system both in the transmission and reflection and the time-delay regimes. Combination of the quantum-limited detection with control over individual fluxons should make the JTL detector suitable for implementation of nontrivial quantum measurement strategies, including conditional measurements and feedback control schemes.

DOI: 10.1103/PhysRevB.73.094504 PACS number(s): 03.67.Lx, 85.25.−j, 03.65.Ta

I. INTRODUCTION

One direction of current efforts aimed at development of mesoscopic solid-state qubits is realization of effective schemes of qubit measurements. Different versions of the qubits which use quantum dynamics of magnetic flux in superconducting loops[1–9] are at the moment among the most advanced solid-state qubits. Practically all of them employ a measurement scheme based on modulation by the measured qubit of the decay rate of the supercurrent of a Josephson junction or a superconducting quantum interference device (SQUID). This process can be viewed as tunneling of a magnetic flux quantum and has several attractive features as the basis for measurement. The most important one is a sufficiently large sensitivity, which comes from strong dependence of the tunneling amplitude on parameters of the tunneling potential controlled by the measured system. There is, however, a practical disadvantage of this approach. Although few-junction structures like SQUIDs can in principle operate as quantum-limited detectors, in the typical detection mode, the supercurrent decay leads to strong energy dissipation, e.g., by bringing the detector into the finite-voltage state. The dissipation perturbs both the system and the detector itself, and makes it impossible to repeat the measurements sufficiently quickly. This prevents realization of nontrivial quantum measurement strategies that are based on continuous measurements or a sequence of successive discrete weak measurements. The goal of this work is to suggest and analyze a flux detector which, similarly to some of the charge detectors, e.g., superconducting Cooper-pair electrometers,[10–12] should operate more naturally in the quantum-limited regime. While still based on tunneling of individual magnetic flux quanta, the detector nevertheless avoids energy dissipation by using ballistic motion of the flux quanta in the Josephson transmission line (JTL).[13] The JTL detector should combine the quantum-limited back action with time resolution sufficient for performing several successive measurements within the typical decoherence time of superconducting qubits. The cost of achieving this is the need for single-flux-quantum (SFQ) support electronics[16] required for operation of this detector. Adaptation of SFQ circuits to qubit applications[17–19] is an important, and not fully solved, problem of development of scalable superconducting qubits.

II. JOSEPHSON TRANSMISSION LINE AS FLUX DETECTOR

As was mentioned in the Introduction, the suggested detector is based on the ballistic motion of fluxons in a JTL which is formed by unshunted junctions with critical currents I_C and capacitances C coupled by inductances L (Fig. 1). The detector can be viewed as the flux analog of the quantum point contact (QPC) charge detectors (see Ref. 20 and references therein) used for measurements of quantum-dot qubits. Both detectors utilize the ability of the measured system to control the ballistic motion of independent particles (electrons in the QPC, fluxons in the JTL detector) through a one-dimensional channel. The JTL detector should, however, provide more control over the propagation of individual fluxons than is possible with electrons in the QPCs. This leads to additional measurement regimes (e.g., time-delay measurements) impossible with the QPC.

The JTL detector uses the fact that the flux $\Phi^{(e)}(x)$ generated by the measured system creates potential $U(x)$ for the

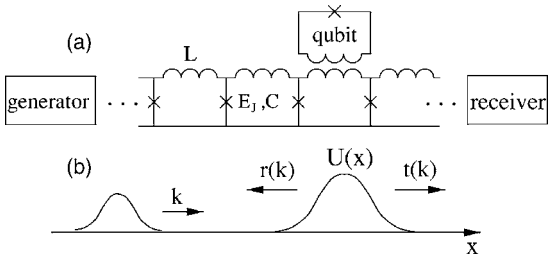

FIG. 1. (a) Equivalent circuit of the flux detector based on the Josephson transmission line (JTL) and (b) diagram of scattering of the fluxon injected into the JTL with momentum k by the potential $U(x)$ that is controlled by the measured qubit. The fluxons are periodically injected into the JTL by the generator and their scattering characteristics [transmission and reflection coefficients $t(k)$ and $r(k)$] are registered by the receiver.

fluxons moving in the JTL (Fig. 1). The fluxons are injected one by one, with period $1/f$, into the JTL by the generator, and are scattered by the potential $U(x)$ localized in some region of the JTL. The injection frequency f is sufficiently low so that only one fluxon at a time moves inside the JTL. The fluxon scattering characteristics, transmission probability or the time delay associated with the motion through the JTL, are registered by the receiver. Since these characteristics depend on the potential $U(x)$ controlled by the measured system, they contain information about the state of this system. For instance, in a simple example of measurement of a qubit strongly coupled to the JTL, the fluxon can be transmitted through the JTL when the qubit is in one state, and reflected back when the qubit is in the other state. In this regime, the outcome of each fluxon scattering gives complete information on the qubit state and the JTL performs strong projective measurement of the qubit. In general, when the coupling to the JTL is weak, the outcome of one scattering event gives only partial information about the measured system.

Quantitatively, Hamiltonian of the uniform JTL can be expressed in terms of the electric charges Q_n and the phases ϕ_n of the Cooper-pair condensate at each of its nodes n:

$$H = \sum_n [Q_n^2/2C + E_J(1 - \cos\phi_n) + E_L(\phi_{n+1} - \phi_n - \phi_n^{(e)})^2]. \tag{1}$$

In this Hamiltonian, $E_J = \hbar I_C/2e$ is the Josephson coupling energy of the junctions, where I_C is the junction critical current, $E_L = (\Phi_0/2\pi)^2/2L$ is the characteristic magnetic energy of inductances L, where $\Phi_0 = \pi\hbar/e$ is the magnetic flux quantum, and $\phi_n^{(e)} = 2\pi\Phi_n^{(e)}/\Phi_0$ is the phase difference across the inductance L of the nth segment induced by the external magnetic flux $\Phi_n^{(e)}$ through this segment. The charges and phases at each node are the conjugate variables that satisfy canonical commutation relations: $[\phi_n, Q_m] = 2ei\delta_{nm}$.

In what follows, we are interested in the regime of small inductances $L \ll \Phi_0/I_C$, when the phase difference across each segment of the JTL is small, and one can replace the phases ϕ_n with a continuous function $\phi(x)$ of dimensionless coordinate $x = n$ along the JTL. (The condition of validity of this approximation is discussed more quantitatively at the end of this section.) In this regime, the JTL is equivalent to a distributed Josephson junction which can act as a uniform ballistic channel for the fluxons. The Hamiltonian (1) reduces in the continuous limit to the standard sine-Gordon Hamiltonian, which can be written as follows:

$$H = 2E_L \int dx \left(\frac{1}{2}[(\partial_\tau\phi)^2 + (\partial_x\phi)^2] + \lambda_J^{-2}(1 - \cos\phi) - \phi^{(e)}(x)\partial_x\phi \right). \tag{2}$$

Here $\tau \equiv ct$ is the time t normalized to the velocity $c = 1/\sqrt{LC}$ of propagation of excitations along the JTL in the absence of Josephson tunneling, and $\lambda_J = (\hbar/2eI_CL)^{1/2}$ is the Josephson penetration length of the junction. We note that in the notations used in Eq. (2) and below, all distances along the JTL, including x and λ_J, are dimensionless, and are measured in units of the cell size a of the JTL (see Fig. 3). Conversion of most equations to absolute units of length can be achieved simply by changing the interpretation of all quantities (e.g., L, C, I_C) from "per cell" to "per unit length."

The commutation relations for the charges and phases give the following equal-time commutation relations for the field $\phi(x,\tau)$ in the Hamiltonian (2):

$$[\phi(x), \partial_\tau\phi(x')] = \beta^2\delta(x - x'), \tag{3}$$

where the parameter $\beta^2 \equiv (4e^2/\hbar)\sqrt{L/C}$ measures the wave resistance $\sqrt{L/C}$ of the JTL in the absence of Josephson tunneling relative to the quantum resistance. Known results for the quantum sine-Gordon model (see, e.g., Ref. 21) show that when $\beta^2 \geq 8\pi$, i.e., $\sqrt{L/C} \geq h/e^2 \simeq 25\ k\Omega$, quantum fluctuations of the field ϕ completely destroy the quasiclassical excitations of the junction. The transition at $\beta^2 = 8\pi$ should be qualitatively similar to the analogous resistance-driven transition in small Josephson junctions.[22] This analogy suggests that the dynamics of the supercurrent flow in the JTL with large wave resistance should be described in terms of tunneling of individual Cooper pairs.[23] While this limit might be reachable in very narrow and thin JTLs of submicrometer width,[24] we assume here a more typical situation, when $\sqrt{L/C}$ is on the order of 10–100 Ω and $\beta^2 \ll 1$. In this case, the JTL supports a number of quasiclassical excitations including, most importantly for this work, topological solitons that carry precisely one quantum of magnetic flux each. The dynamics of such "fluxons" is equivalent to that of stable, in general relativistic, particles[21] with the terminal velocity $c = 1/\sqrt{LC}$ and the mass

$$m \simeq 8\hbar\omega_p/c^2\beta^2 = (2\hbar/e)^{3/2}(I_CL)^{1/2}C, \tag{4}$$

where $\omega_p = (2eI_C/\hbar C)^{1/2} = c/\lambda_J$ is the plasma frequency. Another type of quasiclassical excitation in the JTL is the small-amplitude plasmon waves with frequency

$$\omega(k) = (\omega_p^2 + c^2k^2)^{1/2}, \tag{5}$$

for a wave vector k.

In this work, we are interested in the "nonrelativistic" regime of fluxon dynamics, when the velocity u of its motion is small, $u \ll c$. Equations (4) and (5) show that in this regime, the fluxon kinetic energy $\epsilon = \hbar^2k^2/2m$, where $k = mu/\hbar$, can be made smaller than the lowest plasmon energy $\hbar\omega_p$,

$$\epsilon = \hbar\omega_p(2u/c\beta)^2, \tag{6}$$

so that for $u < c\beta/2$ the fluxon cannot emit a plasmon even when it is scattered by nonuniformities of the JTL potential.[25] Intrinsic dissipation associated with emission of plasmons is then suppressed, and the fluxon motion in the JTL should be elastic, provided that other, "extrinsic," sources of dissipation are also sufficiently weak. Although the JTL operation as the flux detector should be possible for moderately strong fluxon dissipation, the dissipation would prevent the detector from reaching the quantum-limited regime.

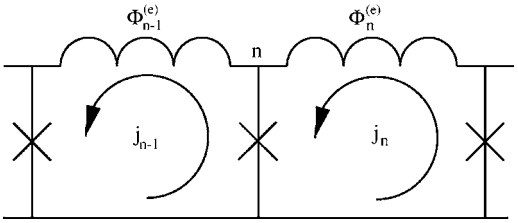

FIG. 2. Equivalence between the magnetic and galvanic coupling to the detector. External fluxes $\Phi_n^{(e)}$ through the JTL cells induce the circulating currents j_n in them which in their turn create the currents $j_n^{(e)}=j_n-j_{n-1}$ through the JTL junctions. The situation would be the same if the currents $j_n^{(e)}$ were injected directly into the JTL junctions by an external system.

The shape of the scattering potential $U(x)$ for fluxons created by the measured system is determined by the convolution of the distribution of the flux $\Phi^{(e)}(x)$ with the distribution of current in each fluxon,[26,27] and can be written as

$$U(x)=\frac{\Phi_0}{2\pi L}\int dx'\frac{\partial\Phi^{(e)}(x')}{\partial x'}\phi_0(x'-x), \tag{7}$$

where $\phi_0(x)$ is the shape of the fluxon which in general can be distorted by the potential $U(x)$ itself. If, however, the potential is smaller than $\hbar\omega_p$, or does not vary appreciably on the scale of the size of the fluxon given by λ_J, the changes in the fluxon shape are negligible, and one can use in Eq. (7) the regular fluxon shape in the uniform case, which in the nonrelativistic limit is $\phi_0(x)=4\tan^{-1}[\exp(x/\lambda_J)]$. One of the implications of Eq. (7) is that the width of the scattering potential $U(x)$ cannot be made smaller than λ_J.

If the measured system is coupled to the JTL not inductively (as in Fig. 1) but galvanically, and injects the current $j^{(e)}(x)$ in the nodes of the JTL, potential created by this current for the fluxons is still given by Eq. (7) if one makes the substitution

$$(1/L)\partial\Phi^{(e)}(x)/\partial x=j^{(e)}(x). \tag{8}$$

The discrete version of Eq. (8) is illustrated in Fig. 2. The external flux $\Phi_n^{(e)}$ through the nth cell of the JTL induces circulating current $j_n=\Phi_n^{(e)}/L$ in this cell. The difference between the currents j_n in the neighboring cells creates the currents $j_n^{(e)}$ through the Josephson junctions of the JTL: $j_n^{(e)}=j_n-j_{n-1}$. In the continuous limit, this relation gives Eq. (8). It implies that direct injection of the currents $j_n^{(e)}$ in the JTL junctions indeed produces the same distribution of phases and currents as magnetic coupling generating the fluxes $\Phi_n^{(e)}$. Throughout this work we assume that the measured system does not inject the net current in the JTL, $\int dx\, j^{(e)}(x)=0$, i.e., the corresponding flux (8) and the potential (7) vanish outside the coupling region: $\Phi^{(e)}(x)\to 0$ for $x\to\pm\infty$.

Although the assumed condition $\beta^2\ll 1$ makes quantum fluctuations of the fluxon shape small, the dynamics of the fluxon as a whole can still be completely quantum. An example of quantum dynamics of fluxons of this type was recently observed experimentally.[28] The JTL detector uses the quantum fluxon dynamics in the potential described by Eqs. (7) and (8). As was mentioned above, operation of the detector requires that the fluxons are injected by the generator into one end of the JTL and observed by the receiver at the other end (Fig. 1). Both of these circuits can be designed following the general principles of the SFQ electronics[16–18] and will not be discussed explicitly here. We simply assume that the ends of the JTL are matched appropriately to these circuits so that the fluxons can enter and leave the JTL without reflection and are injected in the JTL in an appropriate quantum state. This initial state $\psi(x,t=0)$ of an injected fluxon is characterized by the average fluxon velocity u and the wave packet $\psi_0(x)$ defining its position:

$$\psi(x,t=0)=\psi_0(x)e^{ik_0x},\quad k_0=mu/\hbar. \tag{9}$$

As we will see from the discussion in the next section, many properties of the JTL detector are independent of the specific shape of the wave packet $\psi_0(x)$, as long as it is well localized in both coordinate and momentum $\hbar k$. They depend only on the wave-packet width ξ in coordinate space and the corresponding uncertainty of wave vector $\delta k\simeq 1/\xi$. These parameters should satisfy two obvious conditions: $\xi\ll l$, where l is the total length of the JTL, and $\delta k\ll k_0$. We assume a stronger form of the second condition that follows from the requirement that the broadening of the wave packet by $\delta x\simeq\hbar\delta k t/m$ because of the uncertain fluxon velocity during the typical time $t\simeq l/u$ of the fluxon propagation through the JTL is negligible in comparison to the initial width: $\delta x\ll\xi$. We will see below that this requirement is necessary for the quantum-limited operation of the JTL detector in the time-delay mode. The two conditions mean that the width ξ is limited as follows:

$$(l/k_0)^{1/2}\ll\xi\ll l. \tag{10}$$

In cases when it will be necessary to specify the shape of the wave packet $\psi_0(x)$ we will take it to be Gaussian:

$$\psi_0(x)=(\pi\xi^2)^{-1/4}e^{-(x-\bar{x})^2/2\xi^2}, \tag{11}$$

where $\bar{x}$ is the initial fluxon position in the JTL. Besides being well localized as necessary in both the momentum and coordinate space, the wave packet (10) can be obtained as a result of the fluxon generation process that can be implemented naturally with the SFQ circuits. This process consists of the two steps: relaxation of the fluxon to the ground state of a weakly damped and nearly quadratic Josephson potential with the required width ξ of the wave function of the ground state, and then rapid acceleration to velocity u after this potential is switched off.

While the assumed condition $\beta^2\ll 1$ does not preclude the quantum dynamics of fluxons in the JTL, Eq. (4) shows that decreasing β increases the fluxon mass. This makes it more difficult to maintain quantum coherent dynamics of fluxons, which in the case of large mass becomes more susceptible to perturbations. For instance, to avoid the effects of discreteness on the fluxon dynamics in the case of the discrete JTL structure (Fig. 1), the wavelength of its wave function (9) should be larger than the size of one cell. This condition can

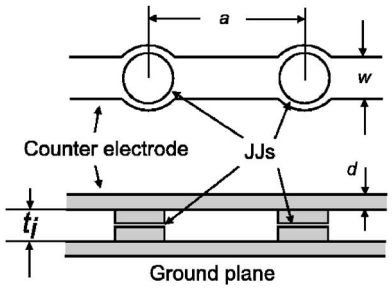

FIG. 3. Geometry of one cell of the multilayer JTL: top view and vertical cross section. Internal layers of the structure are used to create Josephson junctions (JJs), while the two external layers, the ground plane and the counterelectrode, separated vertically by the distance t_i, define inductance L. The length a of the cell is set by the distance between the junctions.

be written as $k_0 \lesssim 1$ and means that the fluxon velocity and kinetic energy cannot be larger than, respectively, $u=\hbar/m = c(\beta^2\lambda_J/8)$ and $\epsilon=\hbar^2/2m$, i.e.,

$$\epsilon = \hbar c \beta^2 \lambda_J/16 = (e^2/C)(\lambda_J/4). \tag{12}$$

We see that both the fluxon velocity u and its kinetic energy ϵ decrease with decreasing β^2 and any external perturbation (e.g., fluctuations of the critical current of the JTL junctions) affects the fluxon motion more strongly at small β. For realistic values of λ_J and β the limitation on the fluxon energy (12) is stronger than (6). The fluxon size λ_J cannot be increased much for reasons of convenience of fluxon manipulation, so that the energy (12) depends essentially only on the junction capacitance C and can be increased only by decreasing the junction size. For the fluxons to be generated with controlled parameters by the generator, the energy (12) should be at least larger than temperature. This means that in practice the JTL can operate as the quantum detector only with submicrometer junctions (see the discussion below). Although the estimate (12) was made for the discrete JTL, the same conclusion would be reached in the case of nominally uniform long Josephson junctions, for which the limitations on the fluxon wave vector k_0 would be set by unavoidable spatial fluctuations of the junction parameters.

We end this section with a discussion of experimental realization of the JTL detector with conventional thin-film "trilayer" fabrication technology of the SFQ circuits. Simplified but sufficiently realistic geometry of one JTL cell in this case is shown in Fig. 3. It contains four superconductor (niobium) films, the lowest and highest of which (ground plane and counter electrode) are used to define inductances, while the two layers in the middle are separated by a very thin layer of insulator (the trilayer structure) and are used to produce the Josephson junctions. Such a discrete multilayer configuration of the JTL is more convenient than a uniform long Josephson junction, since it enables one to optimize separately the junctions and inductances of the JTL, and most importantly, to reduce the effective junction capacitance.

One possible drawback of the discrete configuration could be the parasitic periodic potential $u(z)$ for the fluxons produced by the JTL discreteness (see, e.g., Ref. 29). This potential, however, is negligible when λ_J is not too small, $\lambda_J \geqslant 2$. Indeed, using the Hamilonian (1) and equation for the static distribution ϕ_n that follows from it, we can write the energy E of the static fluxon as

$$E = E_J \sum_n \epsilon_n, \quad \epsilon_n \equiv 1 - \cos\phi_n - \frac{1}{2}\phi_n \sin\phi_n. \tag{13}$$

Applying the Poisson summation formula to this expression, we get in the limit of sufficiently large λ_J:

$$E = E_0[1 + \alpha\cos(2\pi z)], \tag{14}$$

where $E_0=mc^2$ is the fluxon rest energy, z is the fluxon coordinate in units of the JTL period a, and

$$\alpha = \frac{1}{8}\int dy\, \epsilon(y) e^{i2\pi y\lambda_J}. \tag{15}$$

Here $\epsilon(y)$ is a smooth envelope of the discrete distribution ϵ_n (13) associated with the static fluxon ϕ_n. Since $\epsilon(y)$ is smooth in the limit of large λ_J, Eq. (15) implies that the amplitude $\delta\epsilon$ of the z-dependent part of the fluxon energy is exponentially small in λ_J. Specifically, if $\epsilon(y)$ is taken as for the regular "continuous" fluxon $\phi(y)=4\tan^{-1}(e^y)$, we see that

$$\alpha \propto e^{-\pi^2\lambda_J}, \tag{16}$$

and the periodic potential associated with the JTL discreteness is completely negligible for $\lambda_J \geqslant 2$ even on the scale of small fluxon kinetic energy (12). Qualitatively, strong suppression of the fluxon pinning potential with increasing fluxon size λ_J is the result of averaging of JTL properties over the current distribution in the fluxon. Similar averaging should suppress effects of disorder in the parameters of the JTL junctions, which in practice can be made quite small, on the order of few per cent, even before such averaging.

In the multilayer fabrication technology (Fig. 3), the Josephson junctions have a critical current density j_c that can be varied within a wide range, $10-10^4$ A/cm^2, while specific junction capacitance c_J changes only a little, from 30 to 60 fF/μm^2, in this range of j_c's. This means that there is a strong limitation on the minimal junction capacitance C set by the junction diameter D, e.g., $C \simeq 30$ fF for $D \simeq 1.0$ μm. Inductances in the multilayer JTL (Fig. 3) are characterized by the specific inductance per square $\kappa = \mu_0(t_i+2\lambda)$ and parasitic capacitance $c_L \approx \epsilon\epsilon_0/t_i$ per unit area, where t_i is the distance between the external layers and λ is the superconductor penetration depth. For realistic $t_i \approx 0.2-0.4$ μm, κ and c_L are 0.5–0.7 pH and 0.2–0.1 fF/μm^2, respectively.

The discussion leading to Eq. (12) shows that the main requirement on the JTL parameters optimizing its operation as the quantum-limited detector consists in making the junction capacitance C as small as possible. After this, the inductance L can also be reduced as long as this reduction is at least partly compensated by increase in j_c and does not make the characteristic fluxon size λ_J too large. The actual fluxon size is about $4\lambda_J$, and since it is impractical to have significantly more than about 30 cells in the JTL, λ_J is basically fixed within the range from 2 to 3. For relatively small junc-

tion size $D=0.3\ \mu$m and high critical current density $j_c=10\ \mathrm{kA/cm^2}$, the value of λ_J within this range corresponds to $L\simeq 4$ pH, an inductance that is obtained for the width of the superconductor strip $w=1\ \mu$m, and the cell size $a\simeq 5\ \mu$m. For these parameters, the parasitic capacitance c_L gives noticeable contribution (about 30%) to the effective junction capacitance $C\simeq 4$ fF. The propagation velocity along such a JTL is $c\simeq 10^{13}$ cells/s, i.e., 5×10^7 m/s, and the wave resistance is about 30 Ω giving $\beta^2\simeq 0.03$. The useful fluxon velocity in the quantum-limited regime [estimated from Eq. (12)] is 10^{11} cells/s, so that the total time of the fluxon propagation through the JTL (which limits the detector time resolution) is about 0.3 ns. We see that the JTL detector should have very good time resolution even in the quantum-limited regime, but requires in this case JTL parameters that are close to the limit of the current SFQ fabrication technology.

If one abandons the goal of realizing quantum-limited detection, requirements on the JTL become much more routine. A typical set of parameters $D\simeq 1.5\ \mu$m, $j_c=1\ \mathrm{kA/cm^2}$, $w=3\ \mu$m, and $a=10\ \mu$m, produces a JTL with $c\simeq 3\times 10^{12}$ cells/s, wave resistance about 2 Ω, and $\lambda_J\simeq 2$. This should give a detector that is not quantum limited but is very fast and has time resolution on the order of 0.1 ns. As discussed in Sec. V, such a detector could be used in nontrivial schemes of quantum measurement despite the classical dynamics of fluxons in it.

III. MEASUREMENT DYNAMICS OF THE JTL DETECTOR

As discussed above, the measurement by the JTL detector consists qualitatively in scattering of the fluxons in the JTL by the potential controlled by the measured system. This process has the simplest dynamics if the measured system is stationary, and it is convenient to consider it then in the basis of the eigenstates $|j\rangle$ of the system operator (e.g., magnetic flux in the qubit loop in the example shown in Fig. 1) which couples the system to the JTL. In each state $|j\rangle$, the system creates different potential $U_j(x)$ for the fluxons propagating through the JTL. Different realizations $U_j(x)$ of the JTL potential produce different scattering coefficients for injected fluxons: the amplitude $t_j(k)$ of transmission through the JTL, and the amplitude $r_j(k)$ of reflection. Since they depend on the state $|j\rangle$ of the measured system, scattered fluxons carry information about $|j\rangle$.

In general, the process of quantum measurement can be understood as creation of entangled state between the measured system and detector as a result of interaction between them. The states of the detector are quasiclassical and suppress quantum superposition of different outcomes of measurement. The two consequencies of this process are the acquisition of information about the system by the detector and "back-action" dephasing of the measured system—see, e.g., Ref. 30. For the JTL detector, the detector-system entanglement arises as a result of fluxon scattering, and the rates of information acquisition and back-action dephasing can be expressed in terms of the scattering parameters. In this respect, the JTL is very similar to the QPC detector and its characteristics can be obtained following the derivation[20] for the QPC.

Evolution of the density matrix ρ of the measured system in scattering of one fluxon can be obtained by considering first the time dependence of the total wave function of the fluxon injected into the JTL and the wave function $\Sigma_j c_j|j\rangle$ of the measured system:

$$\psi(x,t=0)\sum_j c_j|j\rangle \to \sum_j c_j\psi_j(x,t)|j\rangle. \tag{17}$$

Here the initial fluxon wave function $\psi(x,t=0)$ is given by Eq. (9) and its time evolution $\psi_j(x,t)$ depends on the realization $U_j(x)$ of the scattering potential created by the measured system. Evolution of ρ is obtained then by tracing out the fluxon part of the wave functions (17):

$$\rho_{ij}=c_ic_j^* \to c_ic_j^*\int dx\ \psi_i(x,t)\psi_j^*(x,t). \tag{18}$$

Qualitatively, the time evolution in Eq. (17) describes propagation of the initial wave packet (9) toward the scattering potential and then separation of this wave packet in coordinate space into the transmitted and reflected parts that are well localized on the opposite sides of the scattering region. If we assume that the scattering potential $U(x)$ has a simple shape (for instance, does not have narrow quasibound states) and is nonvanishing only in some small region of size $\eta\ll l$, the time t_{sc} from the fluxon injection to completion of the scattering process is not drastically different from the time l/u of free fluxon propagation through the JTL. Then at time $t>t_{sc}$, the separated wave packets move in the region free from the j-dependent scattering potential and the unitarity of the quantum-mechanical evolution of $\psi_j(x,t)$ implies that the overlap of the fluxon wave functions in Eq. (18) becomes independent of t.

This overlap can be directly found in the momentum representation:

$$\int dx\ \psi_i(x,t)\psi_j^*(x,t)=\int dk|b(k)|^2[t_it_j^*+r_ir_j^*]. \tag{19}$$

Here $b(k)$ is the probability amplitude for the fluxon to have momentum k in the initial state (9), e.g., in the case of the Gaussian wave packet (11),

$$b(k)=(\xi^2/\pi)^{-1/4}e^{-(k-k_0)^2\xi^2/2-i(k-k_0)\bar{x}}. \tag{20}$$

Equations (18) and (19) show that the diagonal elements of the density matrix ρ do not change in the process of scattering of one fluxon, while the off-diagonal elements are suppressed by the factor

$$\nu=\left|\int dk|b(k)|^2[t_i(k)t_j^*(k)+r_i(k)r_j^*(k)]\right|\leqslant 1. \tag{21}$$

The inequality in this relation can be proven as the Swartz inequality for the scalar product in the Hilbert space of "vectors" $\{t_j(k),r_j(k)\}$ weighted by $|b(k)|^2$. The suppression of the off-diagonal elements of ρ due to the interaction with fluxons is a manifestation of the back-action dephasing of the measured system by the JTL detector. If we add the suppression

factors for the fluxons injected into the JTL with frequency f, the rate of this dephasing is obtained as

$$\Gamma_{ij} = -f \ln \left| \int dk |b(k)|^2 [t_i(k) t_j^*(k) + r_i(k) r_j^*(k)] \right|. \quad (22)$$

Equation (22) is similar, but not identical, to the back-action dephasing rate by the QPC detector.[20] The main difference from the QPC is the stage at which the summation over the momentum k is carried out. This difference reflects the fact that in contrast to electrons in the QPC, different k components of the fluxon wave function do not scatter independently. They are constrained by the condition that one fluxon as a whole is either transmitted or reflected by the potential, since scattering events of different fluxons are well separated in time. As we will see below, this difference makes it possible to operate the JTL detector in the time-delay mode that is not possible with the dc-biased QPC detector.

As examples of application of Eq. (22) we consider several specific cases motivated by the measurement regimes discussed below. In one, the phases of the scattering amplitudes are assumed to cancel out from Eq. (22), while the variation of the absolute values of the amplitudes with index j is small. The dephasing rate (22) can be expressed then in terms of the variations $\delta T_j(k)$ of the fluxon transmission probability in different states $|j\rangle$ around some average transmission $T(k)$: $|t_j(k)|^2 = \delta T_j(k) + T(k)$, $\delta T_j(k) \ll T(k)$. In the lowest nonvanishing order in $\delta T_j(k)$ we get

$$\Gamma_{ij} = f \int dk |b(k)|^2 \frac{[\delta T_i(k) - \delta T_j(k)]^2}{8T(k)[1 - T(k)]}. \quad (23)$$

This equation describes the "linear-response" regime of operation of the JTL detector, when its properties follow from the general theory of linear detectors.[30] In particular, the dephasing (23) can be understood as being caused by the back-action noise arising from the randomness of the fluxon transmission and relection processes.

In the "tunnel" limit of weak transmission $|t_j(k)| \ll 1$, and again assuming that the phases of the scattering amplitudes cancel out, Eq. (22) reduces to

$$\Gamma_{ij} = (f/2) \int dk |b(k)|^2 [|t_i(k)| - |t_j(k)|]^2. \quad (24)$$

Both Eqs. (23) and (24) have direct analogs in the case of QPC detectors.[31–33]

As the last example that does not have an analog in QPC physics, we consider the situation when the reflection amplitudes are negligible, $r_j(k) \equiv 0$, and the system-JTL interaction modifies only the phases $\chi_j(k)$ of the transmission amplitudes: $t_j(k) = e^{i\chi_j(k)}$, so that

$$\Gamma_{ij} = -f \ln \left| \int dk |b(k)|^2 e^{i[\chi_i(k) - \chi_j(k)]} \right|. \quad (25)$$

In coordinate representation, this means that the scattering potential affects only the position and, in general, the shape of the transmitted wavepacket. If the width δk of the initial fluxon state in the momentum representation is sufficiently narrow, and the phases $\chi_j(k)$ do not vary strongly over this momentum range, they can be approximated as

$$\chi_j(k) = \chi_j(k_0) - (k - k_0) x_j, \quad x_j \equiv -\chi_j'(k_0). \quad (26)$$

One can see directly that this approximation neglects distortion of the fluxon wave packet in the scattering process, while taking into account its shift x_j along the coordinate axis. This shift can be directly related to the "time delay" τ_j due to scattering: $\tau_j = x_j/u$ (which can be both negative and positive depending on the scattering potential). The dephasing rate (25) can then be conveniently written down in the coordinate representation in terms of the initial fluxon wave packet $\psi_0(x)$:

$$\Gamma_{ij} = -f \ln \left| \int dx \, \psi_0(x - x_i) \psi_0^*(x - x_j) \right|. \quad (27)$$

Equation (27) shows explicitly that the back-action dephasing by the JTL detector arises from the entanglement between the measured system and the scattered fluxons which are shifted in time by an interval dependent on the state of the system. The degree of suppression of coherence between the different states of the measured system is determined then by the magnitude of the relative shift of the fluxon in these states on the scale of the wave packet width. For instance, if the initial fluxon wave packet is Gaussian (11), Eq. (27) gives

$$\Gamma_{ij} = f(x_i - x_j)^2 / 4\xi^2. \quad (28)$$

Back-action dephasing represents only part of the measurement process. The other part is information acquisition by the detector about the state of the measured system. In the case of the JTL detector, this information is contained in the scattering characteristics of fluxons, and the rate of its acquisition depends on specific characteristics recorded by the fluxon receiver. There are at least two different possibilities in this respect. One is to detect the probability of fluxon transmission through the scattering region (or, equivalently, the corresponding probability of the fluxon reflection back into the generator; see Fig. 1). Another possible detection scheme is for the receiver to measure the time delay associated with the fluxon propagation through the JTL. Even if the measured system changes the potential $U_j(x)$ in such a way that the fluxon transmission probability is not affected, potential can still change the fluxon propagation time, which will contain then information about the state of the system. In general, one can have a situation when the information is contained both in the changes of the propagation time and transmission probability, and one needs to detect both scattering characteristics. In this work, we consider only the two "pure" cases of transmission and time-delay detection modes. In general, the goal of realizing quantum-limited detection means that the interaction between the JTL and the measured system, i.e., the fluxon scattering potential $U_j(x)$, should be arranged in such a way that only characteristics of the scattering processes which are actually detected in the particular detection mode contain information about the system. All other characteristics should not carry any informa-

tion. Information in them would be lost in the detector, and can only generate additional dephasing, making it impossible to reach the quantum-limited regime.

A. Transmission detection mode

If the detector records only the fact of the fluxon arrival at the receiver, then only the modulation of the fluxon transmission probability by the measured system conveys information about the system. The information contained in all other features of the scattering amplitudes (e.g., their phases or propagation time) is lost in the receiver. In this case, the rate of information acquisition can be calculated simply by starting with the probabilities of the fluxon transmission and reflection T_j and R_j, when the measured system is in the state $|j\rangle$:

$$T_j = \int dk |b(k)|^2 |t_j(k)|^2, \quad R_j = 1 - T_j. \tag{29}$$

Since the outcomes of successive fluxon scattering event are independent, the probability $p(n)$ to have n out of N incident fluxons transmitted is given by the binomial distribution $p_j(n) = C_N^n T_j^n R_j^{N-n}$. The task of distinguishing different states $|j\rangle$ of the measured system is transformed into distinguishing the probability distributions $p_j(n)$ for different js. Since the number $N = ft$ of scattering attempts increases with time t, the distributions $p_j(n)$ become peaked successively more strongly around the corresponding average numbers $T_j N$ of transmitted fluxons. The states with different probabilities T_j can be distinguished then with increasing certainty. The rate of increase of this certainty can be characterized quantitatively by some measure of the overlap of the distributions $p_j(n)$. While in general there are different ways to characterize the overlap of different probability distributions,[34] the characteristic that is appropriate in the quantum measurement context[35,36] is closely related to "fidelity" in quantum information:[34] $\Sigma_n [p_i(n) p_j(n)]^{1/2}$. The rate of information acquisition (increase of confidence level in distinguishing states $|i\rangle$ and $|j\rangle$) can then be defined naturally as[20]

$$W_{ij} = -(1/t) \ln \sum_n [p_i(n) p_j(n)]^{1/2}. \tag{30}$$

Using the binomial distribution in this expression we get

$$W_{ij} = -f \ln[(T_i T_j)^{1/2} + (R_i R_j)^{1/2}], \tag{31}$$

where the transmission and reflection probabilities are given by Eq. (29).

Equation (31) characterizes the information acquisition rate of the JTL detector in the transmission-detection mode. For an arbitrary detector, the information rate should be smaller than or equal to the back-action dephasing rate, and regime when the two rates are equal is "quantum limited." Comparing Eqs. (22) and (31) one can see that for the JTL detector, indeed,

$$W_{ij} \leqslant \Gamma_{ij}, \tag{32}$$

and equality holds if several conditions are satisfied. First two conditions require that there is no information in the phases of the transmission amplitudes:

$$\phi_j(k) = \phi_i(k), \quad \phi_j(k) \equiv \arg[t_j(k)/r_j(k)], \tag{33}$$

$$\chi_j(k) - \chi_i(k) = \text{const}. \tag{34}$$

The two conditions (33) and (34) have different physical origins. Condition (33) implies that the scattered states contain no information on j that can be used in principle by arranging interference between the transmitted and reflected parts of the wave function.[20] In practical terms, the simplest way to satisfy this condition is to make the scattering potential symmetric $U_j(-x) = U_j(x)$ for all states $|j\rangle$. The unitarity of the scattering matrix for the fluxon scattering in the JTL implies in this case that $\phi_j = \pi/2$ for any j. Condition (34) means that no information on j is contained in the shape and position of transmitted wave packets that would be lost in the fluxon receiver operating in the transmission-detection mode. [Similar condition for the reflected wave packet follows from Eqs. (33) and (34).] In general, condition (34) requires that the spread $\hbar \delta k$ of the initial fluxon state over momentum gives rise to the uncertainty in the fluxon energy $\delta\epsilon \simeq \hbar u \delta k$ that is much smaller than the energy scale Ω of the transparency variation of the scattering potential $U_j(x)$.

One more condition of the quantum-limited operation is that the fluxon transmission probabilities are effectively momentum- and energy-independent in the relevant momentum range:

$$|t_j(k)|^2 = T_j. \tag{35}$$

This condition again requires that $\delta\epsilon \ll \Omega$. It is more restrictive than the corresponding condition for the QPC detector which can be quantum limited even in the case of the energy-dependent transmission probability.[20,37,38] To obtain Eq. (35), one starts from the back-action dephasing rate (22) which can be written as

$$\Gamma_{ij} = -f \ln \int dk |b(k)|^2 [|t_i(k) t_j(k)| + |r_i(k) r_j(k)|]$$

under the conditions (33) and (34). The Swartz inequality for the functions $|t_j(k)|$:

$$[T_i T_j]^{1/2} \geqslant \int dk |b(k)|^2 |t_i(k) t_j(k)|,$$

and the similar inequality for $|r_j(k)|$ show that this Γ_{ij} and the information acquisition rate W_{ij} satisfy the inequality (32). Equality in Eq. (32) can be reached only when

$$|t_j(k)| = \lambda_j t(k), \quad |r_j(k)| = \lambda_j' r(k), \tag{36}$$

where the λ's are some constants, so that the ratios $|t_i(k)|/|t_j(k)|$ and $|r_i(k)|/|r_j(k)|$ are independent of k. Similarly to Eq. (34), Eq. (36) demands that no information about the state of the measured system is contained in the shape of transmitted or reflected wave packets. In general, when both the transmission and reflection probabilities are not small,

the two relations in (36) are incompatible. They have only a trivial solution in which all amplitudes are independent of k in the relevant range of k's, thus proving Eq. (35) for $T_j \sim R_j \sim 1/2$. The transmission and reflection probabilities have roughly the same magnitude when the fluxon energy ϵ is close to the maximum U of the scattering potential. In this case, small spread of ϵ, $\delta\epsilon \ll \Omega$, implies that the range η of the scattering potential $U(x)$ should be small: $\eta \ll \xi$.

Condition (35) of the quantum-limited operation of the JTL detector is not necessary when either $T_j \ll 1$ or $R_j \ll 1$. In this case, one of the relations in (36) reduces to a trivial statement $|r_j(k)| \simeq 1$ or $|t_j(k)| \simeq 1$. The other relation gives then the actual condition of the quantum-limited operation that can be satisfied in principle with an arbitrary k-dependent function $t(k)$ or $r(k)$.

Finally, we show how Eq. (35) applies in the linear-response regime, when the variations δT_j of JTL transparencies between the different states $|j\rangle$ are small and back-action dephasing is given by Eq. (23). Expanding Eq. (31) in δT_j; $T_j = T + \delta T_j$, where all transparencies are defines as in Eq. (29), we get

$$W_{ij} = f(\delta T_i - \delta T_j)^2/[8T(1-T)]. \tag{37}$$

This equation differs from Eq. (23) only by the order in which the integration over momentum is performed. This means that the information and dephasing rates satisfy the inequality (32) and are equal only if the transparency is constant in the relevant momentum range.

In the linear-response regime, each individual fluxon carries only small amount of information, and it is convenient to employ the quasicontinuous description in which the fluxon receiver acts as the voltmeter registering not the individual fluxons, but the rate of arrival of many fluxons, i.e., the voltage $V(t)$ across the junctions of the JTL. The average voltage in the state $|j\rangle$ is

$$\langle V(t)\rangle = fT_j\Phi_0, \tag{38}$$

where $\langle \cdots \rangle$ implies an average over the scattering outcomes and over time t within the fluxon injection cycle. Because of the randomness of the fluxon scattering, the actual voltage fluctuates around the average values (38) even at low frequencies. The voltage fluctuations can be described as the shot noise of fluxons and its spectral density

$$S_V(\omega) = \int d\tau\, e^{-i\omega\tau}[\langle V(t+\tau)V(t)\rangle - \langle V(t)\rangle^2] \tag{39}$$

is constant at frequencies ω below the fluxon injection frequency f. Straightforward calculation similar to that for the regular shot noise shows that this constant is

$$S_0 = fT(1-T)\Phi_0^2, \tag{40}$$

where in the linear-response regime we can neglect small differences δT_j of transparencies between the different states $|j\rangle$ in the expression for noise. This equation shows that in accordance with the general theory of linear quantum measurements, the information rate (37) can be interpreted as the rate with which one can distinguish dc voltage values (38) in the presence of white noise with the spectral density (40).[30,36]

To summarize this subsection, we see that in the most relevant regime $T_j \simeq 1/2$ which maximizes the detector response to the input signal, conditions of the quantum-limited operation of the JTL detector are given by Eqs. (33) and (35). These conditions are satisfied if the scattering potential for the fluxons created by the input signal is symmetric and has the range η smaller that the size ξ of the fluxon wave packet.

B. Time-delay detection mode

Since the range η of the scattering potential (7) cannot be smaller than the fluxon size λ_J, it might be difficult in practice to realize the condition $\eta \ll \xi$ needed for the quantum-limited operation of the JTL detector in the transmission-detection mode. For "quasiclassical" potential barriers that are smooth on the scale of the fluxon wave packet, $\eta \gtrsim \xi$, the "transition" region of energies near the top of the barrier where the reflection and transmission amplitudes have comparable magnitude, is narrow. If the interval $\delta\epsilon$ of the fluxon energies avoids this narrow region, then either transmission or reflection coefficient can be neglected. Ballistic motion of fluxons in this regime still contains information about the potential $U_j(x)$ that can be used for measurement. This information is contained in the time shift τ_j caused by the propagation through the region of nonvanishing potential. Quantum-mechanically, the time-shift information is contained in the phases of the scattering amplitudes. To be specific, we discuss here the regime when the JTL detector is operated in this time-delay detection mode using the transmitted fluxons, i.e., $|t_j(k)| = 1$. In the energy range where $|r_j(k)| = 1$, the same detection process is possible using the reflected fluxons, the advantage of the transmission case being the possibility to make use of the full range of values of the scattering potential: $U_j(x) < 0$ and $U_j(x) > 0$.

For sufficiently smooth potential $U_j(x)$, the phase $\chi_j(k)$ of the transmission amplitude can be calculated in the quasiclassical approximation:

$$\chi_j(k) = \int \frac{dx}{\hbar}\{2m[\epsilon - U_j(x)]\}^{1/2}. \tag{41}$$

If the potential is weak, $U_j(x) \ll \epsilon$, the potential-induced contribution to the phase (41) is

$$\chi_j(k) = -\frac{1}{\hbar u}\int dx\, U_j(x). \tag{42}$$

Under the adopted assumption of quasiclassical potential and vanishing reflection, condition (10) of the negligible broadening of the fluxon wave packet still works in the presence of potential. In this case, one can use the approximation (26) for the phases $\chi_j(x)$ which implies the shift of the wave packet as a whole without distortion. The potential-induced part of the shift $x_j = -\chi_j'(k_0)$ follows from Eq. (41) and has the classical form

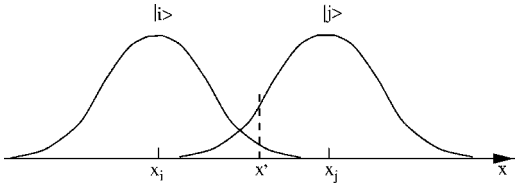

FIG. 4. Illustration of the information acquisition process by the JTL detector in the time-delay mode. The fluxon wave packet is shifted by the distance x_j dependent on the state $|j\rangle$ of the measured system. In conditional description, observation of the fluxon with position x' changes the system wave function according to Eq. (49).

$$x_j = \int dx\left(1 - \frac{u}{u_j(x)}\right), \quad u_j(x) = \{2[\epsilon - U_j(x)]/m\}^{1/2}. \tag{43}$$

For weak potential $U_j(x) \ll \epsilon$

$$x_j = -\frac{1}{2\epsilon}\int dx\, U_j(x). \tag{44}$$

Back-action dephasing rate by the JTL detector in this regime is given by Eqs. (27) and (28). The information about the states $|j\rangle$ contained in the shift τ_j of the fluxon in time or, equivalently, the coordinate $x_j = \tau_j u$, can be read off by distinguishing different shifts x_j against the background of the finite width ξ of the fluxon wave packet $\psi_0(x)$. Since $|\psi_0(x)|^2$ gives the probability of finding the fluxon at coordinate x, this task is equivalent to the task of distinguishing two shifted probability distributions (see Fig. 4) that was discussed above for the transmission-detection mode. Similarly to Eq. (30), we can write the information acquisition rate of the JTL detector in the time-delay mode as follows:

$$W_{ij} = -f \ln \int dx |\psi_0(x - x_i)\psi_0(x - x_j)|. \tag{45}$$

Comparing this to the dephasing rate (27), we see that in general the two rates satisfy the inequality (32) as they should. The rates are equal if the phase of the initial wave packet $\psi_0(x)$ of the injected fluxon is independent of x, i.e., if $\psi_0(x)$ is essentially real. In particular, in the case of the Gaussian wave packet (20), the JTL detector is quantum limited, $W_{ij} = \Gamma_{ij}$, and the two rates are given by Eq. (28). These considerations also imply that the JTL detector in the time-delay mode would lose the property of being quantum limited if the fluxon wave packet spreads noticeably during propagation through the JTL. This process creates a nontrivial x-dependent phase of the wave packet and makes the information acquisition rate smaller than the back-action dephasing rate.

IV. CONDITIONAL EVOLUTION

As is the case with any dephasing, the back-action dephasing by the JTL detector can be viewed as the loss of information. In the regime of the quantum-limited detection, the overall evolution of the detector and the measured system is quantum-coherent and the only source of the information loss is averaging over the detector. For a detector, different outcomes of the evolution are, however, classically distinguishable, and it is meaningful to ask how the measured system evolves for a given detector output. In the quantum-limited regime, specifying definite detector output eliminates all losses of information, and as a result there is no back-action dephasing present in the dynamics of the measured system conditioned on specific detector output.

Conditional description in the quantitative form is obtained (see, e.g., Refs. 36, 39, and 40) by separating in the total wave function the terms that correspond to a specific classical outcome of measurement and renormalizing this part of the wave function so that it corresponds to the total probability of 1. In the case of the JTL detector in the *transmission-detection mode*, for each injected fluxon there are two classically different outcomes of scattering: transmission and reflection of the fluxon. Accordingly, the wave function of the measured system should be conditioned on the observation of either transmitted or reflected fluxon in each cycle of fluxon injection. The evolution of the total wave function "detector+measured system" during the scattering of one fluxon is described by Eq. (17). If conditions (34) and (35) of the quantum-limited detection are satisfied, the transmission and reflection amplitudes are effectively momentum independent.[41] Coordinate dependence of the scattered fluxon wave packets is then the same in different states $|j\rangle$, and can be factored out from the total wave function. The evolution of the measured system can then be conditioned on the transmission and reflection of a fluxon simply by keeping in Eq. (17) the terms that correspond to the actual outcome of scattering. If the fluxon is transmitted through the scattered region or reflected from it in a given injection cycle, amplitudes c_j for the system to be in the state $|j\rangle$ change, respectively, as follows:

$$c_j \to \frac{t_j c_j}{[\Sigma_j |c_j t_j|^2]^{1/2}}, \quad c_j \to \frac{r_j c_j}{[\Sigma_j |c_j r_j|^2]^{1/2}}. \tag{46}$$

It is important to stress that the changes in the coefficients c_j for a system with vanishing Hamiltonian (as we assumed from the very beginning) is unusual from the point of view of Schrödinger equation, and provides quantitative expression of reduction of the wave function in the measurement process. Equations (46) are similar to those obtained in the "bayesian" approach[36] for the QPC detector in the tunnel limit.

If dynamics of the JTL detector is not quantum limited, then information is lost and dephasing is nonvanishing even in conditional evolution. To generalize Eqs. (46) to this case of finite "residual" dephasing, we need to start with Eq. (18) for the change of the density matrix ρ_{ij} of the measured system due to the scattering of one fluxon. To condition this change on the specific outcome of scattering, we limit the trace over the fluxon coordinate to the range containing only transmitted or reflected fluxons. In this way we see that ρ_{ij} changes as

$$\rho_{ij} \to \rho_{ij} \int dk |b(k)|^2 [t_i(k) t_j^*(k)] / \Sigma_j \rho_{jj} T_j, \tag{47}$$

$$\rho_{ij} \to \rho_{ij} \int dk|b(k)|^2[r_i(k)r_j^*(k)]/\Sigma_j \rho_{jj} R_j, \tag{48}$$

if the fluxon is, respectively, transmitted or reflected in a given cycle. Using the discussion of the transmission-detection mode in Sec. III, one can see immediately that the requirements (34) and (35) of the JTL detector being quantum limited are equivalent to the density matrix ρ_{ij} remaining pure in the conditional evolution described by Eqs. (47) and (48).

The above derivation of conditional evolution equations can be repeated with only minor modifications in the *time-delay mode* of the detector operation. In this case, different classical outcomes of measurements are the observed instances of time when the fluxon reaches the receiver, that for convenience can be directly translated into different fluxon positions x at some fixed time. If the fluxon is observed at the position x' in a given injection cycle (Fig. 4), the evolution of the amplitudes c_j of the measured system due to interaction with this fluxon is

$$c_j \to \psi_0(x' - x_j)c_j/[\Sigma_j|c_j\psi_0(x' - x_j)|^2]^{1/2}. \tag{49}$$

Qualitatively, and similarly to the conditional evolution in the transmission mode, the sequence of transformations (49) describes "weak measurement." The system wave function is localized gradually in one of the states $|j\rangle$ with increasing number of the fluxon scattering events which lead to accumulation of information about $|j\rangle$. In contrast to the transmission-detection mode, conditional evolution (49) always remains pure under the simplifying assumptions adopted in this work for the JTL detector: coherent propagation of fluxons with fixed wavepacket $\psi_0(x)$ and the same velocity. Fluctuations in the fluxon generator or finite dissipation in the JTL would create information losses also in this regime.

V. NON-QUANTUM-LIMITED DETECTION

Quantum-limited operation of the JTL detector discussed in the preceding sections requires, in essence, quantum-coherent dynamics of fluxons in the JTL. While this dynamics can be observed experimentally,[28] the task of realizing it is certainly very difficult. From this perspective, it is important that several attractive features of the JTL detector, e.g., large operating frequency and reduced parasitic dephasing during the time intervals between the fluxon scattering, remain even in the non-quantum-limited regime. Although the Josephson junctions of the JTL and those in the "external" parts of the JTL detector (generator and receiver) can give rise to dissipation and dephasing not related directly to measurement, in the JTL geometry (Fig. 1), parasitic dissipation is suppressed due to screening by the supercurrent flow in the JTL junctions.[17]

The dominant deviation from the quantum-limited detection should be associated then with the fluctuations in the fluxon motion. These fluctuations make the dephasing factor ν (21) due to fluxon scattering larger than the amount of information conveyed by the scattering. Some interesting measurement strategies are still possible with the JTL non-

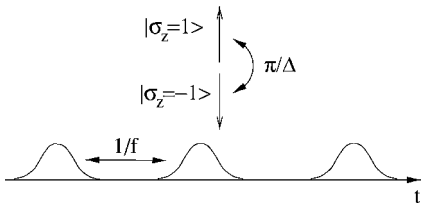

FIG. 5. Schematics of the QND fluxon measurement of a qubit which suppresses the effect of back-action dephasing on the qubit oscillations. The fluxon injection frequency f is matched to the qubit oscillation frequency Δ: $f \simeq \Delta/\pi$, so that the individual acts of measurement are done when the qubit density matrix is nearly diagonal in the σ_z basis, and the measurement back action does not introduce dephasing in the oscillation dynamics.

ideality of this type. The most natural example is the quantum nondemolition (QND) measurements of quantum coherent oscillations in a qubit[42,43] which are designed to make the back-action dephasing by the detector irrelevant. Dynamics of the fluxon scattering in the JTL detector makes it particularly suitable for the "kicked" version of the QND qubit measurements of a qubit[43] or harmonic oscillator.[44]

Consider, for instance, a qubit with the Hamiltonian

$$H = -(\hbar\Delta/2)\sigma_x, \tag{50}$$

which performs quantum coherent oscillations with frequency Δ. The qubit is coupled to the JTL through its σ_z operator, i.e., the states $|j\rangle$ of the preceding sections are the two eigenstates of σ_z. We assume that the Hamiltonian (50) already includes renormalization of parameters due to the qubit-detector coupling. If the qubit oscillations are weakly dephased at the rate $\gamma \ll \Delta$ (e.g., by residual parasitic dissipation in the JTL detector), the time evolution of the qubit density matrix ρ during the time intervals between the successive fluxon scattering events can be written in the σ_z representation as follows:

$$\rho(t) = \frac{1}{2}\left[1 + e^{-\gamma t}\begin{pmatrix} x & -iy \\ iy & -x \end{pmatrix}\right], \tag{51}$$

$$\dot{r} = -i\Delta r, \quad r = x + iy, \tag{52}$$

where $r(t=0) = \pm 1$ depending on whether the qubit starts at $t=0$ from the $\sigma_z = 1$ or $\sigma_z = -1$ state.

The fluxon scattering at times $t_n = n/f$ leads to partial suppression of the off-diagonal elements of ρ:

$$y(t_n + 0) = \nu y(t_n - 0). \tag{53}$$

However, if the fluxons are injected in the JTL with the time interval $1/f$ close to the half period π/Δ of the qubit oscillations (Fig. 5), the qubit density matrix (52) is nearly diagonal at the moments of scattering, $y(t_n) \ll 1$, and suppression (53) does not affect the qubit strongly. Such a QND measurement is possible with the JTL detector operating in any detection mode; to be specific we assume the transmission mode. The dependence of the fluxon transmission probability on the qubit state can be written then as $T + \sigma_z \delta T$, where $\delta T \ll T$ in the "linear-response regime." For quantum-limited detection, the linear-response condition $\delta T \ll T$ implies that

$\nu \to 1$. In the non-quantum-limited case, the back action can be stronger, and we take ν to be arbitrary within the [0,1] interval.

If the frequency f is matched precisely to the qubit oscillations, $f=\Delta/\pi$, the detector does not affect the qubit dynamics at all. If the mismatch is nonvanishing but small, $\delta \equiv \Delta/f-\pi \ll 1$, diagonal elements of ρ (52) evolve quasicontinuously even if suppression factor ν is not close to 1. Equations (52) and (53) give the following equation for this quasicontinuous evolution:

$$\dot{x} = -[(1+\nu)/(1-\nu)](f\delta^2/2)x. \tag{54}$$

In the assumed linear-response regime, the qubit oscillations manifest themselves as a peak in the spectral density $S_V(\omega)$ (39) of the voltage V across the JTL junctions. For $f \simeq \Delta/\pi$ the oscillation peak in $S_V(\omega)$ is at zero frequency. Equations (51) and (54) describing the decay of correlations in the qubit dynamics in the σ_z basis imply that the oscillation peak has Lorentzian shape

$$S_V(\omega) = S_0 + \frac{2\Gamma f^2(\delta T)^2\Phi_0^2}{\omega^2+\Gamma^2}, \tag{55}$$

and the oscillation linewidth Γ is

$$\Gamma = \gamma + \frac{1+\nu}{1-\nu}\frac{(\Delta-\pi f)^2}{2f}. \tag{56}$$

For the quantum-limited detection, $\nu \to 1$, and Eq. (56) reproduces previous results for the QND measurement,[43] if one introduces the back-action dephasing rate $\Gamma_d = f(1-\nu)$. In this case, Eq. (56) is valid for sufficiently small mismatch between the measurement and oscillation frequencies, $|\delta| \ll 1-\nu$. For larger δ, the oscillation peak in the detector output $S_V(\omega)$ moves to finite frequency $\Delta - \pi f$ and the QND nature of the measurement is lost.[42] Equation (56) shows also that in the limit of "projective" measurements $\nu=0$, the broadening of the oscillation peak is weaker, and the peak remains at zero frequency for all reasonable values of the detuning parameter $|\delta| \ll 1$. Therefore, the stronger back-action of the JTL detector is advantageous for the QND measurements of coherent oscillations. The last remark is that although our discussion here assumed that the fluxon arrival times are spaced exactly by $1/f$, Eqs. (55) and (56) should remain valid even in the presence of small fluctuations of the measurement times. These fluctuation can be described by taking into account that the detuning $|\delta|$ cannot be made smaller that the relative linewidth of the fluxon generator.

VI. CONCLUSION

We have suggested and analyzed a ballistic "JTL" detector for the rapid read-out of flux qubits which can be implemented with the present-day SFQ fabrication technology. The detector should combine quantum-limited dynamics with time resolution that is better than the decoherence time of typical flux qubits, making it possible to perform measurements on quantum-coherent qubits. To operate in the quantum-limited regime, the JTL detector requires junctions with submicrometer size, and its time resolution in this regime should reach the range of 0.3 ns. The detector is potentially useful even in the non-quantum-limited regime, when the time resolution can be improved further, and the detector can perform, for instance, QND measurements of coherent oscillations. Although the JTL detector is intended for measurements of flux qubits, it can also can be used for charge qubits, if the information in the charge degrees of freedom is converted into the flux form. This can be done directly in qubits which combine the charge and flux dynamics—see, e.g., Ref. 45.

ACKNOWLEDGMENTS

We would like to thank A. Ustinov for useful discussion. This work was supported in part by ARDA and DOD under the DURINT grant No. F49620-01-1-0439, by the NSF under grant No. DMR-0325551, and by CREST.

[1] J. R. Friedman, V. Patel, W. Chen, S. K. Tolpygo, and J. E. Lukens, Nature (London) **406**, 43 (2000).
[2] D. Vion, A. Aassime, A. Cottet, P. Joyez, H. Pothier, C. Urbina, D. Esteve, and M. H. Devoret, Science **296**, 886 (2002).
[3] Y. Yu, S. Y. Han, X. Chu, S. I. Chu, and Z. Wang, Science **296**, 889 (2002).
[4] I. Chiorescu, Y. Nakamura, C. J. P. M. Harmans, and J. E. Mooij, Science **299**, 1869 (2003).
[5] A. J. Berkley, H. Xu, R. C. Ramos, M. A. Gubrud, F. W. Strauch, P. R. Johnson, J. R. Anderson, A. J. Dragt, C. J. Lobb, and F. C. Wellstood, Science **300**, 1548 (2003).
[6] S. Saito, M. Thorwart, H. Tanaka, M. Ueda, H. Nakano, K. Semba, and H. Takayanagi, Phys. Rev. Lett. **93**, 037001 (2004).
[7] J. Claudon, F. Balestro, F. W. J. Hekking, and O. Buisson, Phys. Rev. Lett. **93**, 187003 (2004).
[8] R. McDermott, R. W. Simmonds, M. Steffen, K. B. Cooper, K. Cicak, K. D. Osborn, S. Oh, D. P. Pappas, and J. M. Martinis, Science **307**, 1299 (2005).
[9] B. L. T. Plourde, T. L. Robertson, P. A. Reichardt, T. Hime, S. Linzen, C.-E. Wu, J. Clarke, cond-mat/0501679 (unpublished).
[10] A. B. Zorin, Phys. Rev. Lett. **76**, 4408 1996.
[11] A. Cottet, A. Steinbach, P. Joyez, D. Vion, H. Pothier, D. Esteve, and M. E. Huber, in *Macroscopic Quantum Coherence and Quantum Computing*, edited by D. V. Averin, B. Ruggiero, and P. Silvestrini (Kluwer, Dordrecht, 2001) p. 111.
[12] D. V. Averin, in *Exploring the Quantum-Classical Frontier: Recent Advances in Macroscopic and Mesoscopic Quantum Phenomena*, edited by J. R. Friedman and S. Han (Nova Science Publishers, New York, 2003), p. 447; cond-mat/0004364.
[13] Another way of avoiding the transition into the dissipative state in the course of measurement is to detect the variations in the junction impedance induced by the measured system. Such "impedance-measurement" schemes (Refs. 14 and 15) enable one to perform the measurements continuously, but they typi-

cally require narrowband coupling between the detector and the measured system, the fact that limits their time resolution.

[14] E. Il'ichev, N. Oukhanski, A. Izmalkov, Th. Wagner, M. Grajcar, H.-G. Meyer, A. Yu. Smirnov, A. M. van den Brink, M. H. S. Amin, and A. M. Zagoskin, Phys. Rev. Lett. **91**, 097906 (2003).

[15] A. Wallraff, D. I. Schuster, A. Blais, L. Frunzio, J. Majer, M. H. Devoret, S. M. Girvin, and R. J. Schoelkopf, Phys. Rev. Lett. **95**, 060501 (2005).

[16] K. K. Likharev and V. K. Semenov, IEEE Trans. Appl. Supercond. **1**, 3 (1991).

[17] V. K. Semenov and D. V. Averin, IEEE Trans. Appl. Supercond. **13**, 960 (2003).

[18] V. K. Kaplunenko and A. V. Ustinov, Eur. Phys. J. B **38**, 3 (2004).

[19] A. M. Savin, J. P. Pekola, D. V. Averin, and V. K. Semenov, cond-mat/0509318 (unpublished).

[20] D. V. Averin and E. V. Sukhorukov, Phys. Rev. Lett. **95**, 126803 (2005).

[21] R. Rajaraman, *Solitons and Instantons* (North Holland, New York, 1982).

[22] A. Schmid, Phys. Rev. Lett. **51**, 1506 (1983).

[23] D. V. Averin, A. B. Zorin, and K. K. Likharev, Sov. Phys. JETP **61**, 407 (1985).

[24] Yu. Koval, A. Wallraff, M. V. Fistul, N. Thyssen, H. Kohlstedt, and A. V. Ustinov, IEEE Trans. Appl. Supercond. **9**, 3957 (1999).

[25] A. Shnirman, E. Ben-Jacob, and B. Malomed, Phys. Rev. B **56**, 14677 (1997).

[26] M. B. Fogel, S. E. Trullinger, A. R. Bishop, and J. A. Krumhansl, Phys. Rev. Lett. **36**, 1411 (1976).

[27] D. W. McLaughlin and A. C. Scott, Phys. Rev. A **18**, 1652 (1978).

[28] A. Wallraff, A. Lukashenko, J. Lisenfeld, A. Kemp, M. V. Fistul, Y. Koval, and A. V. Ustinov, Nature (London) **425**, 155 (2003).

[29] O. M. Braun and Y. S. Kivshar, *The Frenkel-Kontorova Model* (Spinger, Berlin, 2004).

[30] D. V. Averin, in *Quantum Noise in Mesoscopic Physics*, edited by Yu. V. Nazarov (Kluwer, Dordrecht, 2003), p. 229; cond-mat/0301524.

[31] I. L. Aleiner, N. S. Wingreen, and Y. Meir, Phys. Rev. Lett. **79**, 3740 (1997).

[32] Y. Levinson, Europhys. Lett. **39**, 299 (1997).

[33] S. A. Gurvitz, Phys. Rev. B **56**, 15215 (1997).

[34] M. A. Nielsen and I. L. Chuang, *Quantum Computation and Quantum Information* (Cambridge University Press, Cambridge, U.K., 2000), Ch. 9.

[35] W. K. Wootters, Phys. Rev. D **23**, 357 (1981).

[36] A. N. Korotkov, in *Quantum Noise in Mesoscopic Physics*, edited by Yu. V. Nazarov (Kluwer, Dordrecht, 2003) p. 205.

[37] S. Pilgram and M. Büttiker, Phys. Rev. Lett. **89**, 200401 (2002).

[38] A. A. Clerk, S. M. Girvin, and A. D. Stone, Phys. Rev. B **67**, 165324 (2003).

[39] J. Dalibard, Y. Castin, and K. Mølmer, Phys. Rev. Lett. **68**, 580 (1992).

[40] H.-P. Breuer and F. Petruccione, *The Theory of Open Quantum Systems* (Oxford University Press, Oxford, 2002).

[41] Condition (33) of the quantum-limited operation arises from mixing of the transmitted and reflected parts of the wave function and does not directly play a role in the conditional evolution.

[42] D. V. Averin, Phys. Rev. Lett. **88**, 207901 (2002).

[43] A. N. Jordan and M. Buttiker, Phys. Rev. B **71**, 125333 (2005).

[44] R. Ruskov, K. Schwab, and A. N. Korotkov, Phys. Rev. B **71**, 235407 (2005).

[45] J. R. Friedman and D. V. Averin, Phys. Rev. Lett. **88**, 050403 (2002).